

## Photodissociation Dynamics of Formaldehyde Initiated at the $T_1/S_0$ Minimum Energy Crossing Configurations

Benjamin C. Shepler,<sup>†</sup> Evgeny Epifanovsky,<sup>‡</sup> Peng Zhang,<sup>†</sup> Joel M. Bowman,<sup>\*,†</sup>  
Anna I. Krylov,<sup>\*,‡</sup> and Keiji Morokuma<sup>\*,†,§</sup>

Department of Chemistry, University of Southern California, Los Angeles, California 90089, Department of Chemistry and Cherry L. Emerson Center for Scientific Computation, Emory University, Atlanta, Georgia 30322, and Fukui Institute for Fundamental Chemistry, Kyoto University, Kyoto 606-8103, Japan

Received: September 22, 2008; Revised Manuscript Received: November 3, 2008

The photodissociation dynamics of  $H_2CO$  is known to involve electronic states  $S_1$ ,  $T_1$  and  $S_0$ . Recent quasiclassical trajectory (QCT) calculations, in conjunction with experiment, have identified a “roaming” H-atom pathway to the molecular products,  $H_2+CO$  [Townsend; et al. *Science* 2004, 306, 1158.]. These calculations were initiated at the global minimum (GM) of  $S_0$ , which is where the initial wave function is located. The “roaming” mechanism is not seen if trajectories are initiated from the molecular transition state saddle point (SP). In this Letter we identify the minimum energy-crossing configurations and energy of the  $T_1/S_0$  potentials as a step toward studying the multisurface nature of the photodissociation. QCT calculations are initiated at these configurations on a revised potential energy surface and the results are compared to those initiated, as previously, from the  $S_0$  GM as well as the  $S_0$  SP. The product state distributions of  $H_2 + CO$  from trajectories initiated at the  $T_1/S_0$  crossing are in excellent agreement with those initiated at the  $S_0$  GM.

### Introduction

The photodissociation dynamics of formaldehyde have been the subject of intense experimental and theoretical investigations for several decades<sup>1–12</sup> as it plays an important role in environmental, interstellar and combustion chemistry and serves as a prototype for the understanding of photodissociation in larger molecules. The detailed mechanism of the photodissociation dynamics is still unknown; however, it is clear that the process is initiated by photoexcitation of ground-state  $H_2CO$  ( $S_0$ ) to the first excited singlet state ( $S_1$ ) followed by internal conversion to  $S_0$  and intersystem crossing to the first triplet state ( $T_1$ ), which can also intersystem cross to  $S_0$ . Dissociation to ground-electronic-state products does not occur from  $S_1$  and internal conversion to  $S_0$  and intersystem crossing to  $T_1$  are believed to be the mechanisms that lead to these products; ground-state molecular products ( $H_2 + CO$ ) come exclusively from  $S_0$  whereas radical products ( $H + HCO$ ) come from both  $T_1$  and  $S_0$ . On  $S_0$  there is a barrier of 87 kcal/mol to the formation of the molecular products whereas there is no barrier to formation of the radical products on  $S_0$  ( $D_e = 95$  kcal/mol), but there is a barrier on the triplet surface 112 kcal/mol higher in energy than the  $S_0$  global minimum (GM). Ultimately, it will require performing dynamics calculations on these three coupled potential energy surfaces to fully describe this photodissociation.

Quasiclassical trajectory (QCT) calculations of the photodissociation to  $H_2 + CO$  have all been done on  $S_0$  and, until 2004, these were all initiated at the saddle point (SP) transition state (TS) for these products (for the rest of the manuscript we will

refer to this configuration simply as the transition state). In 2004 a joint theoretical-experimental study of the internal energy distribution of these products identified a “roaming” H-atom pathway that by-passes this molecular TS.<sup>7</sup> This roaming pathway is characterized by incipient formation of the radical  $H + HCO$  products where they do not have enough energy to dissociate, but the fragments instead orbit each other followed by H-atom self-abstraction to form  $H_2 + CO$ . The QCT calculations in that study were initiated at the GM of  $S_0$ , which is the equilibrium (EQ) structure of  $H_2CO$ . Further, it was demonstrated that this pathway is not observed if trajectories are initiated at the  $S_0$  SP with the “reaction path” momentum pointed in the direction of the products.

The agreement between theory and experiment to date strongly suggests that it is realistic to initiate the trajectories at the EQ and thus avoid the detailed nonadiabatic dynamics from  $S_1$  and  $T_1$ . However, it is important to determine the limits of validity of this conclusion. A step in this goal is described in this Letter, where we report results of two independent ab initio calculations that have for the first time located the configurations of the minimum energy crossing of the  $T_1$  and  $S_0$  PESs. These crossing points represent a potentially significant path for population to migrate, via spin-orbit coupling, from the excited electronic surfaces back to the ground electronic surface of  $H_2CO$ . The crossings occur at configurations near the transition state separating the *cis*- and *trans*-HOCH isomers on the  $S_0$  surface and thus are quite far from the  $S_0$  GM. The barrier separating *trans*-HOCH from  $H_2CO$  is 86 kcal/mol relative to the  $S_0$  GM, and the TS between *cis*- and *trans*-HOCH is 81 kcal/mol also relative to the  $S_0$  GM. QCT calculations have been initiated at the  $T_1/S_0$  crossing configurations using a slightly modified global PES for  $S_0$  that is based on one reported

<sup>†</sup> Emory University. E-mail: J.M.B., jmbowma@emory.edu.

<sup>‡</sup> University of Southern California. E-mail: A.I.K., krylov@usc.edu.

<sup>§</sup> Kyoto University. E-mail: morokuma@emory.edu.

previously.<sup>13</sup> The results of these new QCT calculations for the molecular and radical channels are compared with calculations initiated, as before, at the H<sub>2</sub>CO GM and also the TS for the molecular products.

Before we describe these calculations we note that two recent articles have reported ab initio calculations of conical intersections between the S<sub>1</sub> and S<sub>0</sub>.<sup>14,15</sup> The lower-energy conical intersection was found to be 107 kcal/mol above the S<sub>0</sub> GM at the MCSCF/6-31G\* level of theory.<sup>15</sup> (B.C.S. and J.M.B. have refined the energy of this second conical intersection in preliminary multireference configuration interaction calculations with an augmented triple- $\zeta$  basis set and found the intersection to be slightly lower at 104 kcal/mol.) Araujo et al.<sup>15</sup> have found that there is a barrier on the PES of S<sub>1</sub> (116 kcal/mol relative to S<sub>0</sub> GM) separating the Franck–Condon region and the lower energy conical intersection that must be passed over or tunneled through. Thus, this conical intersection is unlikely to be of much relevance to the experiments done at a photolysis energy of 87 kcal/mol, where roaming was seen. However, at higher photolysis energies this conical intersection might play a role in the dynamics.

### Methodology and Details of the Calculations

Calculations done at USC (E.E. & A.I.K.) located the GM on S<sub>0</sub> and the local minima corresponding to cis- and trans-HOCH with the coupled cluster method with single and double excitations<sup>16</sup> (CCSD) and employed the cc-pVTZ correlation consistent basis sets.<sup>17</sup> The PES for T<sub>1</sub> was minimized with equation-of-motion CCSD (EOM-CCSD)<sup>18–20</sup> also using the cc-pVTZ basis sets. Two minimum energy S<sub>0</sub>/T<sub>1</sub> crossing points were found using the projected gradient method.<sup>21,22</sup> To refine the energies, a perturbative triples correction via EOM-CCSD(dT)<sup>23</sup> was used. At this higher level of electron correlation, the S<sub>0</sub>/T<sub>1</sub> degeneracy at the CCSD/cc-pVTZ crossing points was lifted. This degeneracy was restored by adjusting the HCOH dihedral angle. Although the resulting geometries are not true minima on the EOM-CCSD(dT) crossing seams, they do represent a good approximation to the true minima. These ab initio calculations were done with the Q-Chem suite of electronic structure programs.<sup>24</sup>

In another independent set of calculations<sup>25,26</sup> done at Emory (P.Z. & K.M.) the internally contracted multireference configuration interaction method with single and double excitations<sup>27,28</sup> plus the multireference analog of the Davidson correction<sup>29</sup> (MRCI+Q) was used. The reference wave functions for the MRCI+Q calculations were obtained from state-specific complete active space self-consistent field (CASSCF) calculations that involved a calculation of 12 electrons in 10 molecular orbitals. The same full-valence active space was employed in the MRCI+Q calculations and the 1s orbitals of C and O were kept doubly occupied in all configurations. In the location of the crossing seams the aug-cc-pVTZ correlation consistent basis sets<sup>17,30</sup> were used. Minima on the seam of crossing were located by constrained geometry optimizations using the Lagrange–Newton method with the aid of numerical MRCI+Q gradients.<sup>31</sup> The energetics of the crossing points were further refined by single point MRCI+Q calculations that employed the aug-cc-pV5Z basis sets. The MOLPRO suite of ab initio programs<sup>32</sup> was used for the MRCI+Q calculations, and the crossing point search was carried out with the HONDO 8.0 program<sup>33</sup> and the SEAM program of Morokuma and co-workers.<sup>34,35</sup>

A global PES for formaldehyde has been reported recently<sup>13</sup> and has been used in several dynamics investigations of the H<sub>2</sub>CO system.<sup>7,9,10,12</sup> This PES has been used in the present QCT

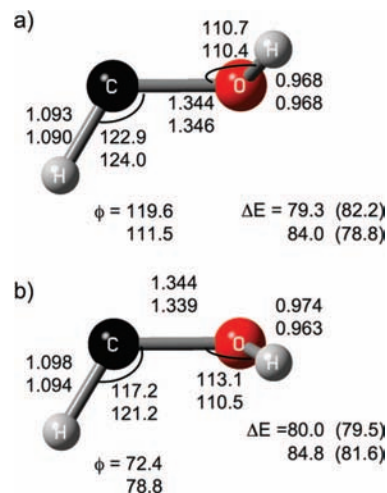


**Figure 1.** Structures (Å) and energies relative to the H<sub>2</sub>CO global minimum (kcal/mol) for the minimum energy crossing points of the T<sub>1</sub> and S<sub>0</sub> surfaces. The trans crossing point is given in Figure 1a and the cis crossing point in Figure 1b. The upper numbers for the structures were computed at the MRCI+Q/aug-cc-pVTZ level of theory and the lower numbers at the EOM-CCSD(dT)/cc-pVTZ level of theory. The upper energy was computed with MRCI+Q/aug-cc-pV5Z, and the lower with EOM-CCSD(dT)/cc-pVTZ. The numbers in parenthesis are the energies from the fitted PES for the corresponding structures.

calculations with adjustments to improve its description of the regions around the minimum crossing points of the T<sub>1</sub> and S<sub>0</sub> surfaces. The modifications were made to the CCSD(T) local fit labeled “fit i” in the original paper.<sup>13</sup> The 15 668 configurations used for this fit were augmented with 1505 ab initio energies, computed at the same CCSD(T)/aug-cc-pVTZ level of theory used in the original work. The configurations for the new energies were obtained from random displacements of the Cartesian coordinates of the minimum energy crossing points and also the recently reported transition state<sup>36</sup> for formation of H<sub>2</sub> + CO from *cis*-HOCH that had not been located at the time of construction of the original PES. The same least-squares procedure and switching functions used in the original fitting were used to join this modified “fit i” to the other five original local fits.

Standard QCT calculations were run on this modified PES and were initiated at four different starting points corresponding to the cis- and trans-T<sub>1</sub>/S<sub>0</sub> minimum crossing points, the molecular channel SP on S<sub>0</sub>, and the global minimum. Trajectories were run at total energies of 35 000, 36 000, 37 000, and 38 000 cm<sup>-1</sup> above the GM. The excess energy was distributed to the Cartesian momenta in all degrees of freedom via random microcanonical sampling subject to the constraint of zero total angular and linear momentum. Microcanonical sampling was chosen, in part, because the T<sub>1</sub>/S<sub>0</sub> minimum crossing points are not stationary points and so normal mode sampling was not an option. A total of 5000–10 000 trajectories were run for each energy and at each of the four starting points with a time step of 0.048 fs and integrated for a maximum of 400 000 steps using the velocity–Verlet integrator. More trajectories were run for the lower energies to have enough completed trajectories for analysis (50% of trajectories have not dissociated after 400 000 time steps at 35 000 cm<sup>-1</sup> and less than 1% did not dissociate at 38 000 cm<sup>-1</sup>).

### Results and Discussion

The structures of the trans- and cis-minimum energy crossing points are presented in Figure 1, at the indicated level of theory

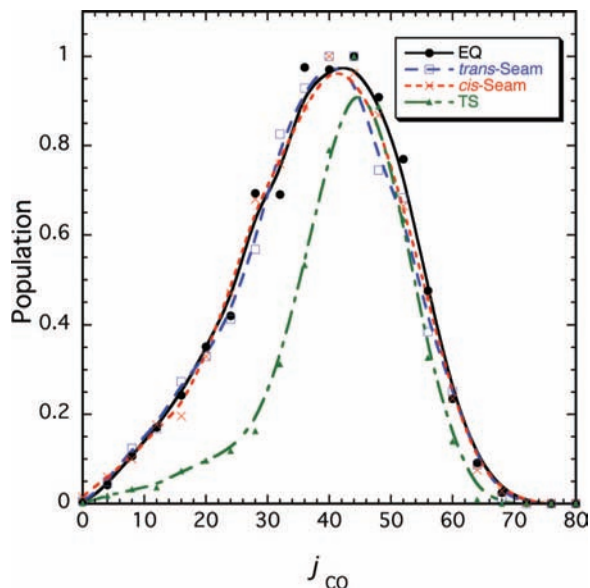


**Figure 2.** CO rotational distribution for trajectories with 37 000  $\text{cm}^{-1}$  total energy (corresponding to a 31 156  $\text{cm}^{-1}$  photolysis energy). The four curves are for trajectories initiated at the formaldehyde global minimum (EQ), the trans-minimum energy crossing point (Trans-Seam), the cis-minimum energy crossing point (Cis-Seam), and the transition state connecting the global minimum to the molecular products (TS).

and basis. The structures of the crossing points resemble the transition state connecting *trans*- and *cis*-HOCH on the  $S_0$  surface and the HOCH  $T_1$  minimum,<sup>25</sup> which have dihedral angles of roughly  $90^\circ$  and  $100^\circ$ , respectively, compared to the dihedral angles of roughly  $110^\circ$  and  $80^\circ$  for the *trans*- and *cis*-crossing points. The energy of the minimum crossing points is similar to the energy of this nearby *cis*–*trans* TS and the  $T_1$  minimum. At the CCSD(T)/aug-cc-pVTZ level of theory the TS lies 80.8 kcal/mol above the global minimum while the  $T_1$  minimum is 76.9 kcal/mol computed at the MRCI+Q/aug-cc-pV5Z level of theory.<sup>25</sup> The  $T_1/S_0$  crossing points have potential energies between 79–85 kcal/mol. For comparison, the energies of the fitted PES for the MRCI+Q and EOM-CCSD configurations are also given in Figure 1.

Product state distributions for the molecular products  $\text{H}_2 + \text{CO}$  are given in Figures 2 (the CO rotational distribution) and 3 (the  $\text{H}_2$  vibrational distribution) at a photolysis energy of 31 156  $\text{cm}^{-1}$  (37 000  $\text{cm}^{-1}$  relative to the EQ) initiated at the configurations indicated. As seen, the distributions initiated from the EQ and the  $T_1/S_0$  crossing geometries are essentially identical. Thus, the mechanism for the formation of molecular products is the same whether the trajectories are initiated from the  $T_1/S_0$  minimum energy seams or the EQ geometry. Animations show that trajectories initiated at the  $T_1/S_0$  seam sample the *cis*- and *trans*-HOCH wells for a period of time before finding the deeper  $\text{H}_2\text{CO}$  well. Trajectories generally remain in this  $\text{H}_2\text{CO}$  well long enough to randomize the energy before reacting to produce  $\text{H}_2 + \text{CO}$  either via the molecular SP TS or roaming pathway. (Note there is a transition state connecting *cis*-HOCH to the molecular products, but it is energetically inaccessible at the photolysis energies considered here. At higher photolysis energies this additional pathway may become significant.)

Differences between the product distributions for trajectories initiated from the EQ and TS configurations have been discussed already in depth in a number of previous investigations;<sup>7,9,10</sup> however, we note that the present distributions, though quite

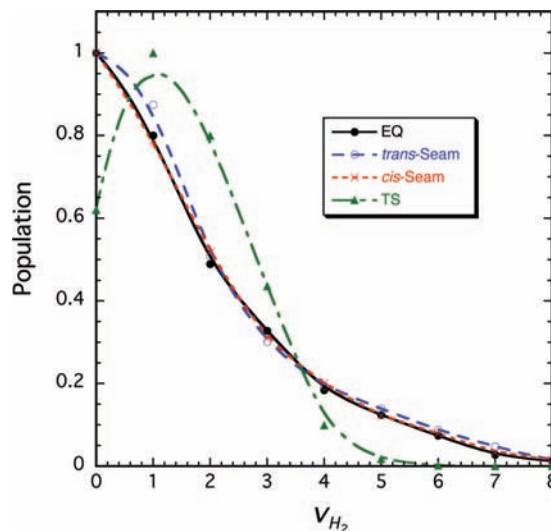


**Figure 3.**  $\text{H}_2$  vibrational distribution for trajectories with 37 000  $\text{cm}^{-1}$  total energy (corresponding to a 31 156  $\text{cm}^{-1}$  photolysis energy). The four curves are for trajectories initiated at the formaldehyde global minimum (EQ), the trans-minimum energy crossing point (Trans-Seam), the cis-minimum energy crossing point (Cis-Seam), and the transition state connecting the global minimum to the molecular products (TS).

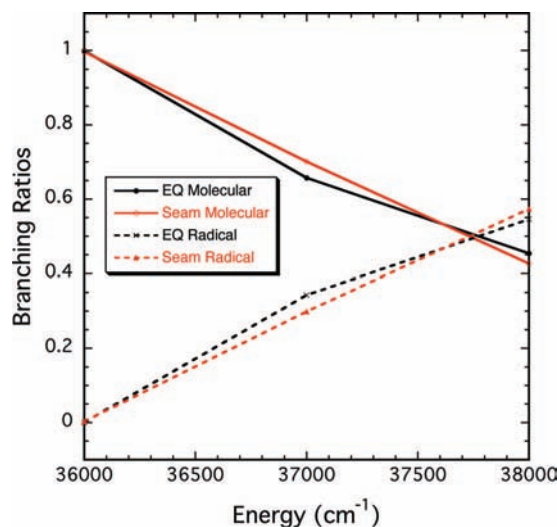


**Figure 4.** Branching ratios of molecular ( $\text{H}_2 + \text{CO}$ ) and radical ( $\text{H} + \text{HCO}$ ) products for formaldehyde unimolecular dissociation. The energies on the x-axis represent the excess energy in the system (total energy minus the zero-point energy of  $\text{H}_2\text{CO}$ ).

similar to previous ones, show some quantitative differences. This is attributable to subtle differences in the two potential surfaces, and different procedures for the sampling of the initial conditions. In the previous studies the C–H bond was activated in the initial conditions of the EQ trajectories and this resulted in a slightly higher incidence of roaming trajectories and this is consistent with production of slightly more rotationally cold CO and vibrationally hot  $\text{H}_2$ . The TS trajectories do not sample the roaming pathway and this accounts for the colder  $\text{H}_2$  vibrational distributions and hotter CO rotational distributions for the TS trajectories, as discussed in detail elsewhere.<sup>7,9,10</sup>

Finally, the branching ratios for the molecular and radical channels for GM and seam initiated trajectories are shown in Figure 4 (the branching ratio at 35 000  $\text{cm}^{-1}$  for  $\text{H} + \text{HCO}$  is zero, and so this energy is not shown). The standard procedure of removing trajectories that produce products with less than their required zero-point energy (ZPE) has been employed. As



seen, there is good agreement for these two sets of trajectories. That there should be this good agreement is not obvious because  $\text{H}_2 + \text{CO}$  can only be produced (at the energies considered here) from the  $\text{H}_2\text{CO}$  well, but trajectories initiated at the seam can produce  $\text{H} + \text{HCO}$  directly from the *cis*- or *trans*-HOCH wells. In fact a small number of such trajectories do exist; however, they tend to produce HCO with less than ZPE. If all trajectories are considered at  $37\,000\text{ cm}^{-1}$  then  $\text{H} + \text{HCO}$  produced from the HOCH well accounts for 18% of the total radical products. However, the average internal energy of the HCO produced from the HOCH well is 5.7 kcal/mol compared to 8.0 kcal/mol for HCO produced from the  $\text{H}_2\text{CO}$  well. Therefore, when including the ZPE constraint only 6% of the radical products are produced from the HOCH well at this energy. Of course, some of this difference could be influenced by the way in which the initial conditions were sampled and further study is warranted.

## Conclusions

Minimum-energy crossing points have been located between the  $T_1$  and  $S_0$  surfaces of formaldehyde using state-of-the-art *ab initio* calculations. The seam of crossing between  $T_1$  and  $S_0$  lies in the region of the HOCH isomers of formaldehyde. Quasiclassical trajectory calculations performed on a modified analytical PES for  $S_0$  find no differences in the product state distributions of the molecular products or in the molecular/radical branching ratios whether the trajectories were initiated at the minimum-energy crossing points on the seam or at the  $\text{H}_2\text{CO}$  equilibrium geometry.

The present work provides further insight into the full photodissociation mechanics of formaldehyde. However, a complete description of this process necessarily requires dynamics to be run on at least three coupled potential energy surfaces for  $S_1$ ,  $T_1$  and  $S_0$ . Construction of accurate global potentials for  $T_1$  and  $S_1$  are in progress.

**Acknowledgment.** J.M.B. and B.C.S. thank the Department of Energy (DE-FG02-97ER14782), as does A.I.K. (DE-FG02-05ER15685). A.I.K. and J.M.B. also acknowledge that this work is partially conducted under the auspices of the iOpenShell Center for Computational Studies of Electronic Structure and Spectroscopy of Open-Shell and Electronically Excited Species supported by the National Science Foundation through the CRIF: CRF CHE-0625419 + 0624602 + 0625237 grant. K.M. acknowledges partial support from grants from AFOSR (FA9550-04-1-0080 and FA9550-07-1-0395) and computer time provided by a grant under the DoD-High Performance Computing Program and by the Research Center for Computational Science, Obozaki, Japan as well as by the Cherry L. Emerson Center for Scientific Computation, Atlanta, GA.

## References and Notes

- (1) Jaffe, R. L.; Hayes, D. M.; Morokuma, K. *J. Chem. Phys.* **1974**, *60*, 5108.
- (2) Moore, C. B.; Weisshaar, J. C. *Annu. Rev. Phys. Chem.* **1983**, *34*, 525.

- (3) Schinke, R. *J. Chem. Phys.* **1986**, *84*, 1487.
- (4) Green, W. H.; Moore, C. B.; Polik, W. F. *Annu. Rev. Phys. Chem.* **1993**, *43*, 591.
- (5) van Zee, R. D.; Foltz, M. F.; Moore, C. B. *J. Phys. Chem.* **1993**, *99*, 1664.
- (6) Feller, D.; Dupuis, M.; Garrett, B. C. *J. Chem. Phys.* **2000**, *113*, 218.
- (7) Townsend, D.; Lahankar, S. A.; Lee, S. K.; Chambreau, S. D.; Suits, A. G.; Zhang, X.; Rheinecker, J.; Harding, L. B.; Bowman, J. M. *Science* **2004**, *306*, 1158.
- (8) Yin, H.-M.; Nauta, K.; Kable, S. H. *J. Chem. Phys.* **2005**, *122*, 194312.
- (9) Bowman, J. M.; Zhang, X. *Phys. Chem. Chem. Phys.* **2006**, *8*, 321.
- (10) Farnum, J. D.; Zhang, X.; Bowman, J. M. *J. Chem. Phys.* **2007**, *126*, 134305.
- (11) Suits, A. G.; Chambreau, S. D.; Lahankar, S. A. *Int. Rev. Phys. Chem.* **2007**, *26*, 585.
- (12) Troe, J.; Ushakov, V. *J. Phys. Chem. A* **2007**, *111*, 6610.
- (13) Zhang, X.; Zhou, S.; Harding, L. B.; Bowman, J. M. *J. Phys. Chem.* **2004**, *108*, 8980.
- (14) Simonsen, J. B.; Rusteika, N.; Johnson, M. S.; Sølling, T. I. *Phys. Chem. Chem. Phys.* **2008**, *10*, 674.
- (15) Araujo, M.; Lasorne, B.; Bearpark, M. J.; Robb, M. A. *J. Phys. Chem. A* **2008**, *112*, 7489.
- (16) Purvis, G. D., III.; Bartlett, R. J. *J. Chem. Phys.* **1982**, *76*, 1910.
- (17) Dunning, T. H., Jr. *J. Chem. Phys.* **1989**, *90*, 1007.
- (18) Sekino, H.; Bartlett, R. J. *Int. J. Quantum Chem.* **1984**, *Suppl 18*, 255.
- (19) Stanton, J. F.; Bartlett, R. J. *J. Chem. Phys.* **1993**, *98*, 7029.
- (20) Krylov, A. I. *Annu. Rev. Phys. Chem.* **2008**, *59*, 433.
- (21) Bearpark, M. J.; Robb, M. A.; Schlegel, B. *Chem. Phys. Lett.* **1994**, *223*, 269.
- (22) Epifanovsky, E.; Krylov, A. I. *Mol. Phys.* **2007**, *105*, 2515.
- (23) Manohar, P. U.; Krylov, A. I. *J. Chem. Phys.*, submitted for publication.
- (24) Shao, Y.; Molnar, L. F.; Jung, Y.; Kussmann, J.; Ochsenfeld, C.; Brown, S. T.; Gilbert, A. T. B.; Slipchenko, L. V.; Levchenko, S. V.; O'Neill, D. P.; DiStasio, R. A.; Lochan, R. C.; Wang, T.; Beran, G. J. O.; Besley, N. A.; Herbert, J. M.; Lin, C. Y.; Van Voorhis, T.; Chien, S. H.; Sodt, A.; Steele, R. P.; Rassolov, V. A.; Maslen, P. E.; Korambath, P. P.; Adamson, R. D.; Austin, B.; Baker, J.; Byrd, E. F. C.; Dachsel, H.; Doerksen, R. J.; Dreuw, A.; Dunietz, B. D.; Dutoi, A. D.; Furlani, T. R.; Gwaltney, S. R.; Heyden, A.; Hirata, S.; Hsu, C. P.; Kedziora, G.; Khallilulin, R. Z.; Klunzinger, P.; Lee, A. M.; Lee, M. S.; Liang, W.; Lotan, I.; Nair, N.; Peters, B.; Proynov, E. I.; Pieniazek, P. A.; Rhee, Y. M.; Ritchie, J.; Rosta, E.; Sherrill, C. D.; Simmonett, A. C.; Subotnik, J. E.; Woodcock, H. L.; Zhang, W.; Bell, A. T.; Chakraborty, A. K.; Chipman, D. M.; Keil, F. J.; Warshel, A.; Hehre, W. J.; Schaefer, H. F.; Kong, J.; Krylov, A. I.; Gill, P. M. W.; Head-Gordon, M. *Phys. Chem. Chem. Phys.* **2006**, *8*, 3172.
- (25) Zhang, P. Ph.D. thesis, Emory University, 2005.
- (26) Zhang, P.; Morokuma, K. Submitted for publication.
- (27) Knowles, P. J.; Werner, H.-J. *Chem. Phys. Lett.* **1988**, *145*, 514.
- (28) Werner, H.-J.; Knowles, P. J. *J. Chem. Phys.* **1988**, *89*, 5803.
- (29) Langhoff, S. R.; Davidson, E. R. *Int. J. Quantum Chem.* **1974**, *8*, 61.
- (30) Kendall, R. A.; Dunning, T. H., Jr.; Harrison, R. J. *J. Chem. Phys.* **1992**, *96*, 6796.
- (31) Koga, N.; Morokuma, K. *Chem. Phys. Lett.* **1985**, *119*, 371.
- (32) MOLPRO, version 2006.1, a package of *ab initio* programs, H.-J. Werner, P. J. Knowles, R. Lindh, F. R. Manby, Schütz, and others, see <http://www.molpro.net>.
- (33) Dupuis, M.; Chin, S.; Marquez, A. CHEM-station and HONDO. In *Relativistic and Electron Correlation Effects in Molecules and Clusters*; Malli, G. L., Ed.; NATO ASI Series; Plenum Press: New York, 1992.
- (34) Cui, Q.; Morokuma, K.; Stanton, J. F. *Chem. Phys. Lett.* **1996**, *263*, 46.
- (35) Dunn, K. M.; Morokuma, K. *J. Chem. Phys.* **1995**, *102*, 4904.
- (36) Schreiner, P. R.; Reisenauer, H. P.; Pickard, F. P.; Simmonett, A. C.; Allen, W. D.; Matyus, E.; Csaszar, A. G. *Nature* **2008**, *453*, 906.

JP808410P